Weather and Climate Extremes 34 (2021) 100404

Contents lists available at ScienceDirect

Weather and Climate Extremes

journal homepage: www.elsevier.com/locate/wace

2019/2020 drought impacts on South America and atmospheric and oceanic influences

Mariah Souza Gomes [a], Iracema Fonseca de Albuquerque Cavalcanti [a,*], Gabriela V. Müller [b,c]

[a] Centro de Previsão de Tempo e Estudos Climáticos- Instituto Nacional de Pesquisas Espaciais (CPTEC/INPE), Brazil
[b] Consejo Nacional de Investigaciones Científicas y Técnicas (CONICET), Argentina
[c] Centro de Estudios de Variabilidad y Cambio Climático (CEVARCAM), Universidad Nacional del Litoral, Santa Fe, Argentina

A R T I C L E I N F O

Keywords:
Drought
South America
Impacts
Precipitation anomalies
Atmosphere and ocean features

A B S T R A C T

The 2019/2020 drought in South America caused many impacts on several sectors, as agriculture, water resources and environment, which are reported here. Besides, there is a discussion about anomalies in the atmosphere and ocean during the analyzed period. In a regional scale, there was a reduction of humidity flux over the continent, and in a large scale, the occurrence of different processes could have contributed to the dry conditions. There was a persistent pattern of west-east convection anomalies in the tropical Pacific that could be related to the steady conditions observed over South America and southeast South Atlantic from September 2019 to March 2020. The extreme positive phase of the Indian Ocean Dipole during 2019 austral spring was another event that could have influenced temperature and precipitation in South America through a wavetrain from the Indian Ocean to the South American continent. The Sudden Stratospheric Warming that occurred in September 2019 induced the negative phase of the Southern Annular Mode in December, which generated subsidence over the subtropics and affected the precipitation over South America. In addition, from September 2019 to March 2020, the heating observed in the stratosphere propagated to the troposphere over South America. Ocean indices from 1982 to 2020 are analyzed in the context of dry conditions in the continent and it was observed the relations with AMO, PDO, IOD and El Niño 3.4. From September 2019 to March 2020, there were positive SST anomalies in all oceans, mainly in the North Atlantic Ocean, which could have contributed also to subsidence over South America through a meridional circulation, as seen in other cases. At the end of the studied period, the development of La Niña extended the situation of reduced precipitation in Southern Brazil.

1. Introduction

Recurrent extreme events, particularly droughts, are growing in importance to the scientific community, given that such events have direct and indirect impacts on humans and all other living beings around the planet. Droughts are complex slow-onset phenomena (Wilhite, 2012) caused by reduced precipitation. As widely known, droughts are classified into meteorological, agricultural, hydrological, and socio-economic, according to their intensity, duration, and impacts on different sectors (Wilhite and Glantz, 1985). However, this is not the only classification that exists. In fact, defining and classifying droughts is complicated because of the multiple dimensions of the phenomenon (Wilhite and Glantz, 1985). It is even difficult to determine and predict its onset or end. Something all types of droughts have in common is that they originate from a deficiency of precipitation that affects the availability of water to society, a group or an activity (Wilhite and Glantz, 1985).

According to NASA (2020a), the second most severe drought in South America (SA) since 2002 took place from 2019 to 2020, only after the event recorded in the east of Brazil and Venezuela from 2015 to 2016. In their report, NASA (2020a) noted that the first drought signs were observed in shallow groundwater storage from satellite gravimetry data by mid-2018 over the SE of Brazil and spreading over areas in Paraguay, Bolivia, and later over northern Argentina, to cover the entire continent by October 2020. In contrast with most parts of the continent, the trimester January-February-March 2020 in SE Brazil was the wettest in almost twenty years (Vasconcellos and Souza, 2020). The anomalies reached almost all SE Brazil, with the exception of São Paulo State that

; SA, South America.

* Corresponding author. INPE, Av. dos Astronautas, 1758. São José dos Campos, S.P., Brazil.
E-mail address: iracema.cavalcanti@inpe.br (I.F.A. Cavalcanti).

https://doi.org/10.1016/j.wace.2021.100404
Received 14 June 2021; Received in revised form 24 September 2021; Accepted 29 November 2021
Available online 30 November 2021

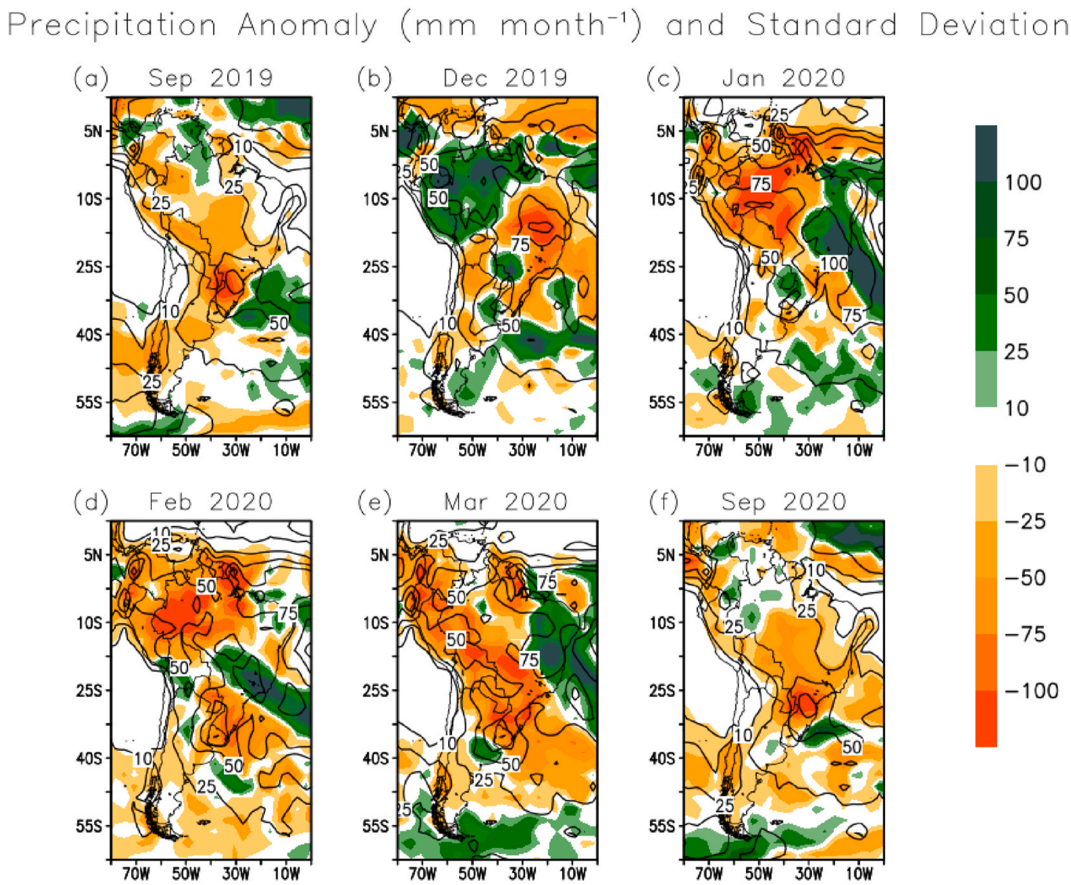

Fig. 1. Precipitation anomalies (mm.month^{-1}) and standard deviation for (a) SEP 2019, (b) DEC 2019, (c) JAN 2020, (d) FEB 2020), (e) MAR 2020, (f) SEP 2020.

had similar behavior of the Southern Region of Brazil, i.e., negative precipitation. These positive anomalies extended to the Atlantic Ocean, in a NW-SE direction, indicating a greater role of the oceanic SACZ (Vasconcellos and Souza, 2020).

The long dry period in the center and south of SA had extensive impacts on the social, economic and environmental sectors. The impacts of this phenomenon represent millions of dollars in losses to the affected countries. Yields of winter corn crops were low and the delay in spring rainfall caused farmers to delay soybean sowing. Very low water levels in major South American rivers (Paraguay, Parana, and La Plata) hindered and even impeded navigation and transport, affected tourism as well as local and regional economies through reduced fishing. Water level in the Paraguay river during 2020 was among the lowest recorded in the past 100 years (AP News, 2020) and the low water level in the Parana River was the most critical in the past 50 years (INA, 2020). Consequently, transportation had to be restricted in some sections of this river and with delayed cargo and ships carrying smaller-than-normal loads, millions of dollars in commerce were lost (BCR, 2020) The shipment of cereals and minerals down the Paraná-Paraguay Waterway, which functions as an outlet to the Atlantic Ocean, was seriously affected (Marengo et al., 2021). Moreover, low water in the Paraná River also affected the river ecosystem and other essential activities such as fishing and water purification (BCR, 2020).

The lack of precipitation and low water levels contributed to the intensification of transboundary fires in Brazil, Bolivia, Paraguay and Argentina. Many of the affected areas got under unusually intense extensive fires (NASA, 2020a). The Pantanal, a vast floodplain in SA, in the countries of Brazil, Paraguay and Bolivia, is among the largest wetlands in the world. The unusually active 2019 fire season (July to October), and low rainfall during the 2020 rainy season (December to April) faced by the Pantanal meant that these wetlands never had a chance to recharge (NASA, 2020b). That made it easier for the fires to continue burning during the first half of the calendar year, when fire activity is typically minimal in this region. But it was in July and August, the beginning of the dry season, when fire activity increased, which until the beginning of September 2020, had charred approximately 24,000 square kilometers of the Pantanal, i.e., more than 10 percent of its area (NASA, 2020b).

Some of the major impacts in South American countries are described in the following sections.

1.1. Agriculture and livestock

a. Argentina

The most affected areas in the first semester of 2020 were northwestern Argentina, the north of the province of Santa Fe, the center-east of Entre Rios province and several areas in the province of Buenos Aires, as reported by the Buenos Aires Grain Market (BCBA, 2020). Wheat was the most affected crop during the studied drought, mainly in the center of Argentina, according to the July 2020 report of the Rosario Stock Exchange (BCR, 2020), when over 1 million hectares had already been affected by the lack of rainfall in the country. The remaining five million hectares devoted to wheat were left unproductive until the sowing season of maize and soybean.

b. Southern Brazil

According to the Department of Rural Economics (Deral, 2020), agriculture experienced major losses in the three southern states – i.e., Santa Catarina, Rio Grande do Sul, and Parana, with over 40% of the area affected (CEMADEN, 2020). Soybean was the most affected crop in

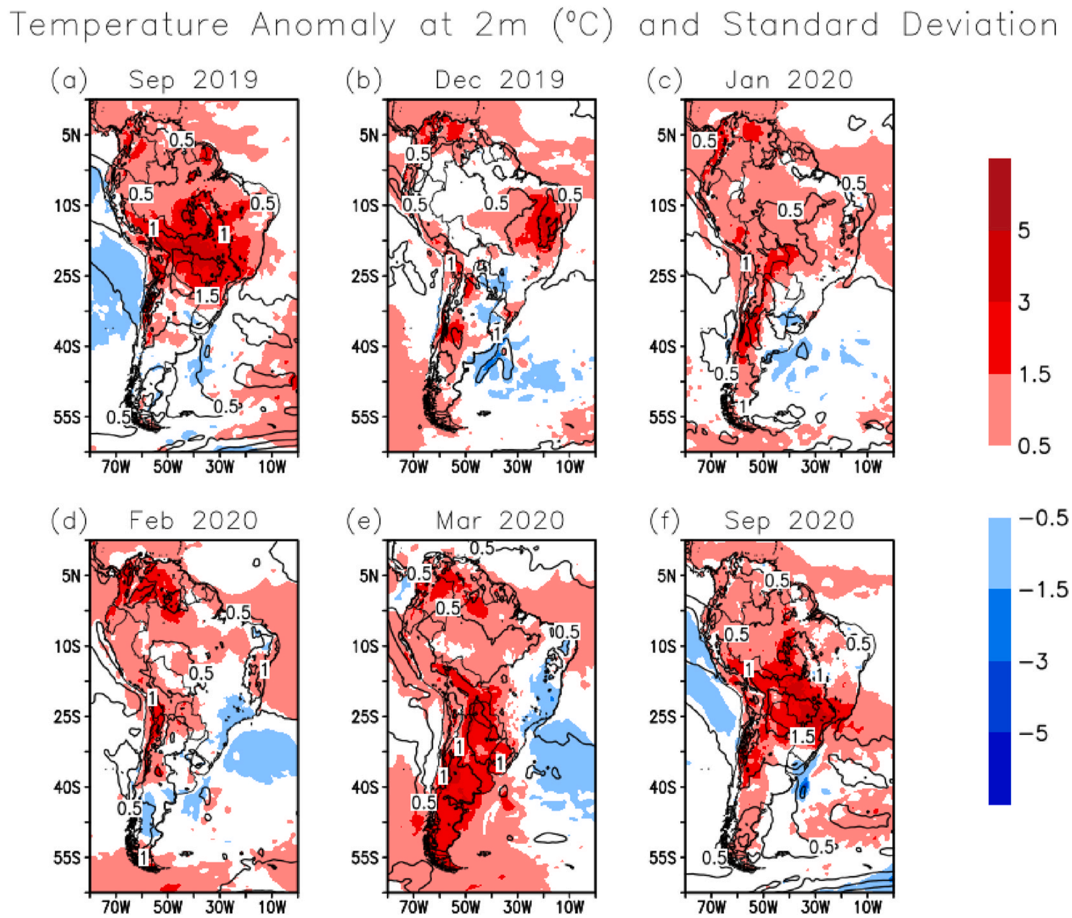

Fig. 2. Temperature anomalies at 2 m (^{0}C) and standard deviation for (a) SEP 2019, (b) DEC 2019, (c) JAN 2020, (d) FEB 2020), (e) MAR 2020, (f) SEP 2020.

Rio Grande do Sul, with yield losses above 70% in some areas and from 57 to 40% in other areas compared to previous year's yields. Maize losses were the greatest in the state of Santa Catarina, reaching 43% in some localities, and 15% in the state of Parana, compared to previous year's yields (EPAGRI/CEPA, 2020). Rio Grande do Sul also experienced poor maize yields (CEMADEN, 2020). Bean was the most affected late planting crop, with losses close to 27% (compared to 2018/2019 yields) in the state of Parana (EPAGRI/CEPA, 2020). In this context many state farmers were forced to apply to the PROAGRO assistance program (CEMADEN, 2020).

c. Paraguay

Soil moisture deficits affected maize crop in April 2020. Planting of some wheat varieties was also impeded by the lack of water and high temperature (DMH, 2020). In the center and north of the country planting of pea, oats, and sugar cane (DMH, 2020) was delayed because of the lack of precipitation. Family farmers were affected by losses in crops that were at the growing stage in August 2020, i.e., maize, bean, watermelon, and melon. According to DMH (2020), yields of extensive crops, such as wheat, also dropped markedly in quantity and quality because of the drought.

d. Uruguay

Loss caused by the 2019–2020 drought in the agricultural and cattle ranching sector were estimated at US$ 546 million, mainly because of soybean failure, but also because of decreased yields in maize and sorghum (MAGyP, 2020). Besides the need for importing livestock supplies, drought impacts included reduced production and productivity of beef cattle, and the death in livestock (OPYPA, 2020).

1.2. Water resources

a. Argentina

During the first semester of 2020, the Parana River reached its lowest level since 1971 (INA 2020), which implied enormous industrial and transport logistics problems. Commodities export was greatly affected as it uses fluvial transport. In the Rosario port hub, where about 80% of the country's farm exports are loaded, losses were estimated at US$244 million in the first four months of the year 2020 (BCR, 2020).

b. Southern Brazil

The rainfalls below normal that started in 2019 resulted in reduced river streamflow and strong impact on communities. According to CEMADEN (2020), the lowest levels at reservoirs occurred in April 2020, impacting hydropower generation and water supply mainly in three states of southern Brazil -Paraná, Santa Catarina and Rio Grande do Sul. Hydropower plants located at the Parana and Iguazu rivers saw their lowest historical levels (CEMADEN, 2020).

c. Paraguay

Low water levels were recorded in all water courses in the country, and particularly in the Paraguay river (DMH, 2020). Such levels caused the interruption of waterways and the consequent economic losses, as 80% of Paraguayan trade – equivalent to about US$ 2 200 million yearly-is transported fluvially. Land transportation was not able to meet

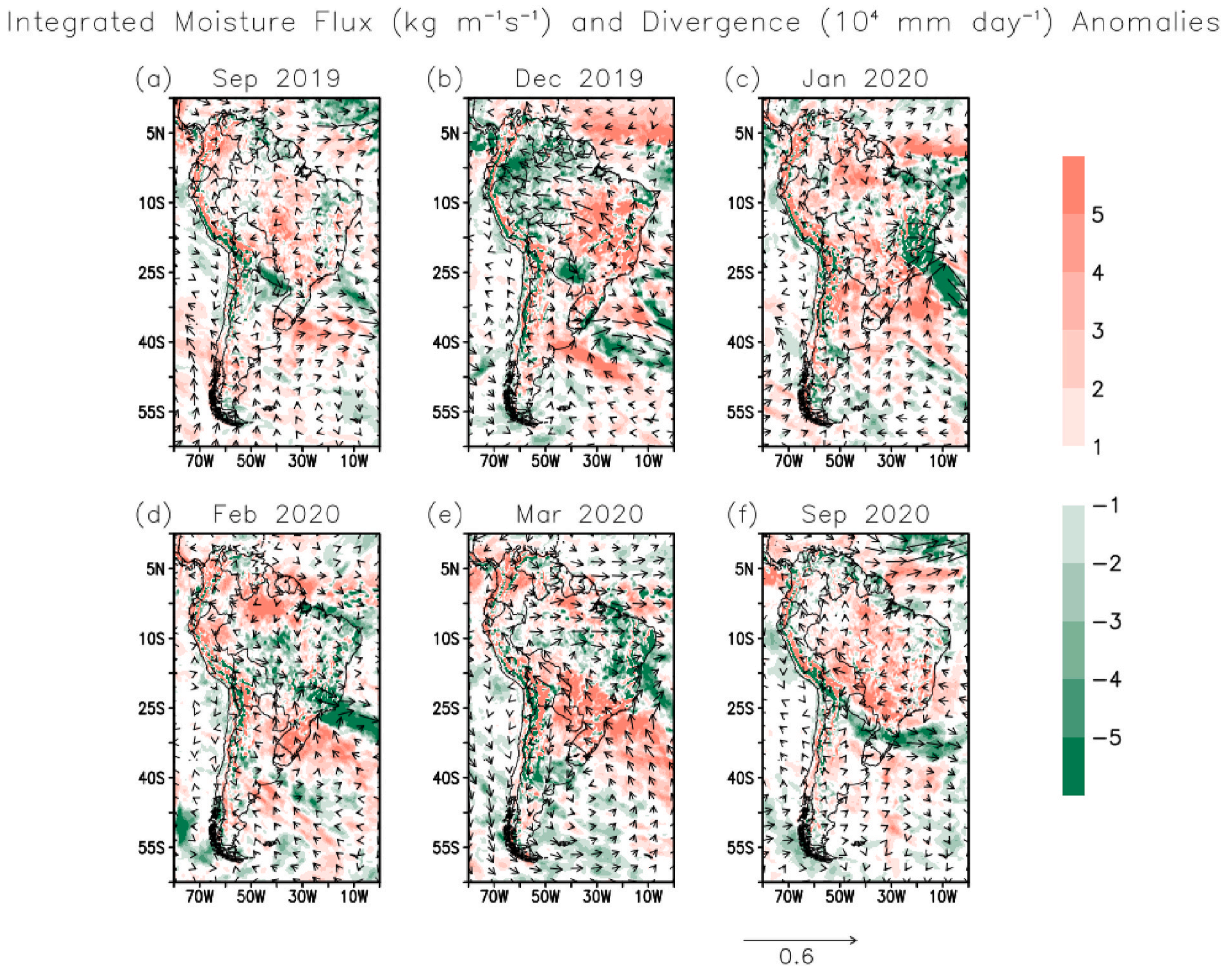

Fig. 3. Vertically integrated humidity flux (kg. m^{-1}.s^{-1}) and divergence (mm/day) for (a) SEP 2019, (b) DEC 2019, (c) JAN 2020, (d) FEB 2020), (e) MAR 2020, (f) SEP 2020.

export commitments and the country lost several commodities contracts. Import was also affected, and products from Argentina were acquired at a much higher cost (La Nación, 2020).

1.3. Fires

a. Argentina

Only in the northeast of the country, 400,000 ha burnt in 2020 (SNMF, 2020) and 1.101.267 ha in the north (MAGyP, 2020). Some of these fires were related to agricultural practices, however the extensive drought caused those fires to expand over large territories. In September 2020, fires peaked (MAGyP, 2020) and spread all over the regions under drought. In the north of the country, fires also caused agricultural and livestock losses of about 7 000 million dollars.

Because of the fires, an increased amount of nutrients reached the low water courses and water bodies in the La Plata basin, which caused eutrophication, and consequent cyanobacteria blooms. Water purification plants collapsed in the city of La Plata in November 2020 (Clarín, 2020), and the use of water from the La Plata River was forbidden because of its toxicity (Telam, 2020).

b. Brazil

Although the 2019 fires in the Amazonia had high media exposition worldwide, in 2020 there were over 90,000 fires, 45% above the average of the past ten years. The Pantanal was also affected by fire, with almost 22,000 fires (INPE, 2020). Satellite data revealed that by the beginning of September 2020, more than 10% of the Pantanal area had been affected. In fact, 2020 was a year with the greatest number of fires along the country, since they began to be monitored in 1999 (INPE, 2020).

Meteorological droughts are caused by persistent anomalies in large-scale circulation patterns, usually caused by sea surface temperature anomalies or other remote drivers (Schubert et al., 2004). Considering the impacts caused by the most severe drought in SA in the past 20 years (NASA, 2020a), besides the above documentation, we analyzed the atmospheric and oceanic conditions during the 2019/2020 drought period and discussed the processes that contributed to the extreme precipitation anomalies in large areas of SA. In section 2, we describe the data and method of analyses, in section 3 there is a discussion about the precipitation, temperature and humidity flux anomalies, and in section 4, the large-scale features in the Southern Hemisphere atmosphere and in the North Atlantic Ocean SST are analyzed and linked to the drought over SA. We explore the convection anomalies in the Indian Ocean/-Indonesia/West Pacific, the wavetrains and centers of action over Pacific and South Atlantic Oceans, the North Atlantic SST, the occurrence of the Sudden Stratospheric Warming (SSW), the occurrence of La Niña and the humidity flux over SA. We conclude in section 5, comparing this drought with those of 2014 and 2015.

2. Data and method

Monthly precipitation from the Global Precipitation Climatology Project (GPCP 2.3), obtained from NOAA/OAR/ESRL/PSD and

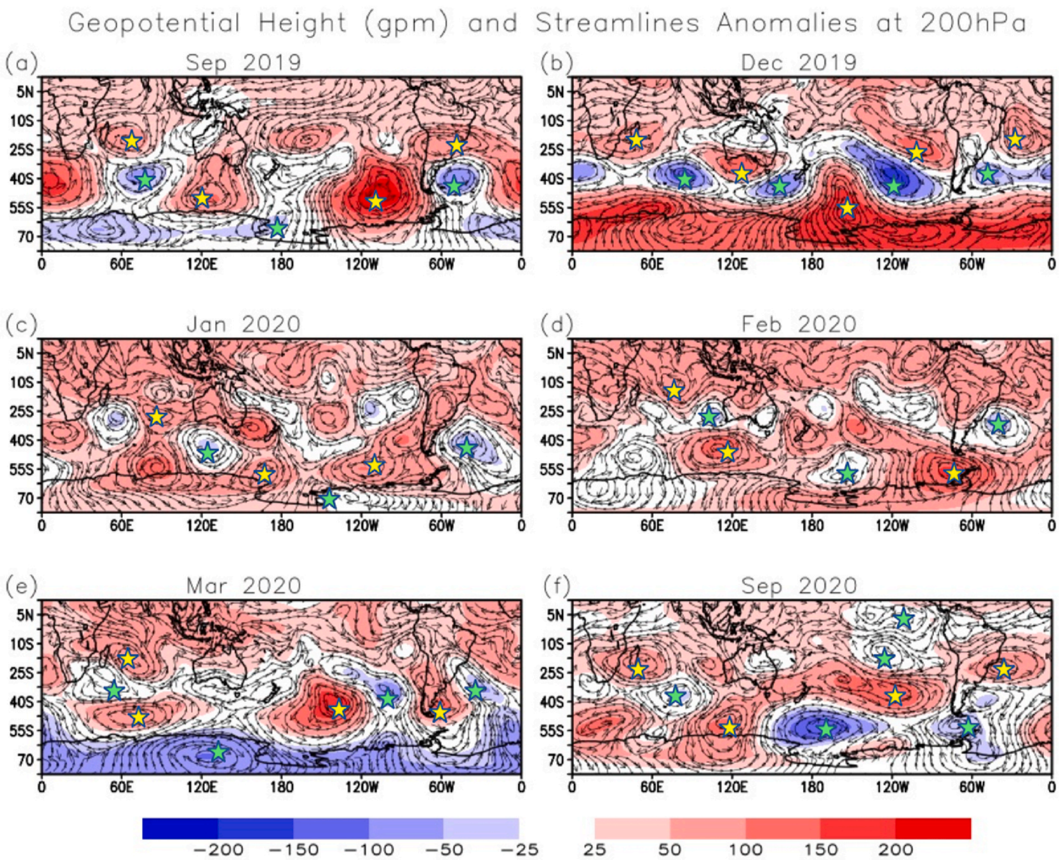

Fig. 4. Geopotential height anomalies (gpm) and streamlines at 200 hPa of (a) SEP 2019, (b) DEC 2019, (c) JAN 2020, (d) FEB 2020), (e) MAR 2020, (f) SEP 2020.

described in Adler et al. (2018) were used to identify the areas where there were dry conditions over SA during 2019/2020. The atmospheric conditions during the period were analyzed using temperature at 2 m, temperature, zonal, meridional and vertical wind components, from 1 000 hPa to 200 hPa, humidity from 1 000 hPa to 500 hPa, geopotential heigh at 200 hPa, obtained from monthly ERA-5 reanalysis- ECMWF (Hersbach et al., 2020). Outgoing Longwave Radiation (OLR) provided by Climate Data Record (CDR)-NOAA (Lee, 2018) was used to analyze convection in the Indian Ocean/Indonesia/West Pacific. The Sea Surface Temperature (SST) ocean conditions were analyzed using the Extended Reconstructed Sea Surface Temperature-version 5 dataset derived from the International Comprehensive Ocean-Atmosphere Dataset (ICOADS), (Huang et al., 2017). Monthly anomalies of all variables were obtained using the monthly 1981 to 2010 climatology period.

SST indices, such as Pacific Decadal Oscillation (PDO), Atlantic Multidecadal Oscillation (AMO), Indian Ocean Dipole (IOD) and El Niño 3.4 were obtained from NOAA ESRL Physical Sciences Laboratory: https://psl.noaa.gov/gcos_wgsp/Timeseries. AMO is unsmoothed, detrended from the Kaplan SST V2. PDO is the leading PC of monthly SST anomalies in the North Pacific Ocean, derived from OI.v2 SST fields. Dipole Mode Index (DMI), which represents the Indian Ocean Dipole (IOD), is calculated from SST anomaly at (10^0 S –10^0 N, 50^0 E –70^0 E) minus (10^0 S - 0^0, 90^0 E - 110^0 E) area averaged using HadISST. El Niño is calculated as SST anomalies in the area (5^0 N–5^0S;170^0 W–120^0 W) from HadISST.

Besides the analyses of the whole period of extreme drought that occurred from spring 2019 to spring 2020 over SA, six months were chosen to analyze the spatial atmospheric conditions. These were months when large areas of the continent were affected with high negative rainfall anomalies: September (SEP) and December (DEC) 2019, and January (JAN), February (FEB), March (MAR), SEP 2020.

3. Precipitation, temperature and humidity flux conditions over South America

The austral summer (DEC-JAN-FEB) is the climatological rainy season in large areas of SA, associated with the South American Monsoon System (SAMS, Marengo et al., 2012; Carvalho and Cavalcanti, 2016). However, during the summer 2019–2020, below normal precipitation was registered in the majority of the continent and the negative anomalies presented higher values than the standard deviation (Fig. 1b,c,d). In DEC (Fig. 1b), except over western Amazon, there were dry conditions in many regions of SA. The drought was intense in Amazonia, central-western and parts of southeastern SA in JAN (Fig. 1c) and FEB (Fig. 1d). During these two months, there were positive precipitation anomalies over part of southeastern Brazil, extending to the ocean, in a pattern consistent with the oceanic South Atlantic Convergence Zone (SACZ), when the convective band is extended from SE to the ocean and there is dry condition in Amazonia (Carvalho et al., 2004). The same configuration was discussed by Vasconcellos and Souza (2020), who analyzed the rainy trimester of JAN-FEB-MAR 2020 over SE Brazil. Different from this configuration, the continental SACZ is wider and extends to the Amazon region (Carvalho et al., 2004; Rosa et al., 2020). The dominant mode of precipitation variability in the summer, over South America, presents opposite anomalies between the monsoon region and the northwest and southeast SA (Grimm and Zilli, 2009; Cavalcanti et al., 2017; Barreto et al., 2019). During the 2019/2020 summer, although there was anomalous positive precipitation over southeast Brazil in JAN and FEB, and negative anomalies to the south and to northwest, the negative anomalies extended over the whole Amazon, in a different pattern, compared to the normal variability and to the continental SACZ events.

Previous to the summer months, dry conditions were established in SEP 2019 (Fig. 1a) over SA, and after the summer, high negative

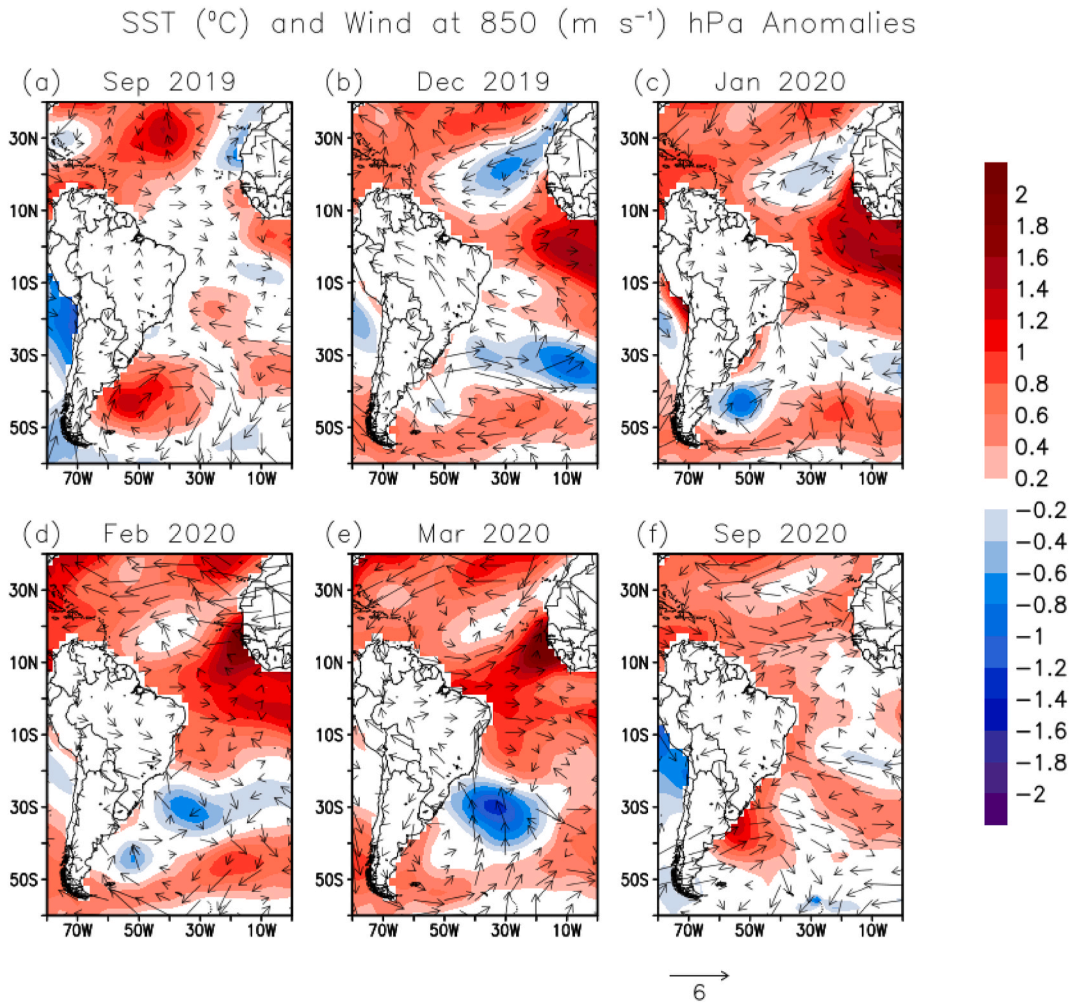

Fig. 5. SST anomalies (^{0} C) and wind vectors anomalies (m/s) at 850 hPa.

precipitation anomalies extended from the Amazon region to southeast SA in MAR 2020 (Fig. 1e) affecting these regions and also the central region. The drought continued in some regions of the continent until the spring 2020, as shown in SEP 2020 (Fig. 1f), very similar to the precipitation anomalies of SEP 2019 (Fig. 1a). In northern Argentina and southern Brazil, the persistence of below normal rainfall was evident particularly in SEP 2019, MAR and SEP 2020. Considering the anomalies in the whole Argentina, 2020 was considered the fifth driest year of the whole time series from 1961 to 2020, and the driest year in Argentina since 1995 (SMN, 2021).

During the analyzed period, the months of SEP (2019, 2020) and MAR 2020 registered a large extension of high positive temperature anomalies at 2 m, above the standard deviation in many areas (Fig. 2a,e, f). The high temperatures and the lack of precipitation contributed to the fires that occurred during 2019–2020 in several areas of SA, in Brazil (Aragão et al., 2020) and Argentina (SNMF, 2020; MAGyP, 2020). It should also be noted that 2020 was the second warmest since 1961 in Argentina (SMN, 2021), which may have considerably enhanced the drought effects that affected the region.

The anomalous precipitation conditions during the summer months were linked to the anomalous vertically integrated humidity flux (Fig. 3), which showed reduced flux towards southeast Brazil in DEC (Fig. 3b), and flux anomalies directed to SE and to the ocean in JAN (Fig. 3c) and FEB (Fig. 3d), consistent with the precipitation band extended over the ocean in these months. There is humidity divergence over the dry areas and convergence over SE and the oceanic SACZ. The normal conditions during these months exhibit humidity flux from the Amazon region directed toward Southeast Brazil or toward La Plata Basin (Arraut et al., 2012; Martinez and Dominguez, 2014), many times associated with the Low Level Jet (LLJ) occurrence (Marengo et al., 2004). In SEP 2019, 2020 (Fig. 3a,f) the flux anomalies were very small over SA, and in MAR 2020 the flux anomalies were opposite to the climatological direction, indicating a reduction in the humidity flux over the continent. Consistent with the dry conditions, there were anomalous divergence of humidity in large areas of SA.

4. Large scale features

The Southern Hemisphere (SH) atmospheric circulation anomalies during these months are displayed in the geopotential anomalies at 200 hPa (Fig. 4). Numbers three and four extratropical wavetrains are identified in the patterns, and the common feature is the negative anomaly center over southwestern South Atlantic, close to southeastern SA, from SEP 2019 to MAR 2020. This center is part of the wavetrain that crosses the Pacific Ocean, although with different configurations from SEP 2019 to SEP 2020. Over the continent there were persistent positive geopotential anomalies, during this period, indicating higher thickness and higher temperature than climatology in the atmosphere, at the same time that the colder air of the anomalous trough was persistent over southwest South Atlantic, extended to South and SE coast in DEC and MAR respectively (Fig. 4). In JAN, FEB and MAR, the negative center displaced northwards over the ocean, near the coast, and contributed to the establishment of the precipitation band over southeast and northeast Brazil (Fig. 1c,d,f and Fig. 4c,d,f). These monthly

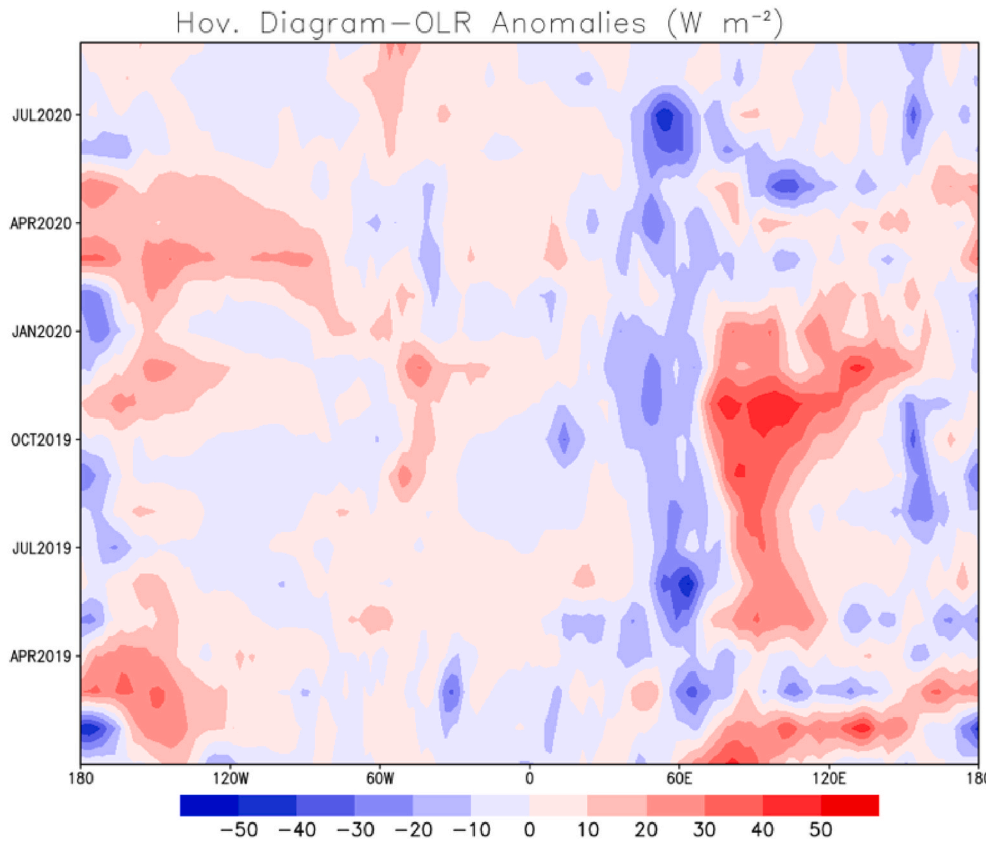

Fig. 6. Hovmöller diagram of OLR ($W.m^{-2}$) averaged in latitudes of 10 S–10 N.

average anomalies suggest that the synoptic systems like cold fronts were intensifying the oceanic SACZ, while the other regions of the continent were dry. The establishment of the cyclonic anomaly over South Atlantic Ocean linked to a wavetrain over the Indian and Pacific Oceans, during the trimester of DEC-JAN-FEB, was also identified in Vasconcellos and Souza (2020), associated with excessive precipitation over Southeast Brazil. Besides, they showed an influence of the Atlantic SST on this oceanic SACZ configuration, through correlations between SST in the subtropical South Atlantic and precipitation anomalies over South America. Consistent with those analyses, from DEC 2019 to MAR 2020 there are negative SST anomalies in this region of Atlantic Ocean and positive SST anomalies in large areas of the North and Tropical Atlantic (Fig. 5).

To investigate why the anomalous negative center over southwest South Atlantic was persistent, as well as the maintenance of positive geopotential anomalies over the continent, the conditions over the Pacific Ocean were analyzed. It is known that the Madden-Julian Oscillation (MJO) affects the SACZ trough interactions tropics-extratropics by the Pacific South America (PSA) wavetrain or through the zonal tropical displacement of convection (Mo and Paegle, 2001; Cunningham and Cavalcanti, 2006; Carvalho et al., 2011). The typical MJO configuration over Equatorial Pacific is a west-east pair of anomalous negative and positive OLR, meaning anomalous convection, which displaces eastwards in an intraseasonal timescale (Madden and Julian, 1972). However, during 2019/2020, this pair remained stationary for more than six months over the Indian Ocean and Indonesia and did not displace eastwards (Fig. 6). This seems to affect the usual triggering of the PSA wavetrains that affect SA, and could have collaborated to the stationarity of the cyclonic center over southwestern South Atlantic Ocean, which affected areas of SE in JAN and FEB and areas of NE in MAR (Fig. 4). This cyclonic center is part of a wavetrain observed from the steady convection anomaly over the Indian Ocean (Fig. 6) during the period. Vasconcellos and Souza (2020) linked the divergence at high levels over the Indian Ocean to the presence of a wavetrain to SA in the trimester of JAN-FEB-MAR (2020). Consistent with that discussion, wavetrains are observed in the monthly analyses of geopotential height and streamlines anomalies from the Indian Ocean to SA (Fig. 4).

Another feature that can be related to the drought during the period, was the occurrence of the Sudden Stratospheric Warming (SSW). Lim et al. (2019) related the weakening of the SH polar vortex to droughts in Australia, showing that during these periods there were strong positive temperature anomalies and reduced precipitation over Australia. The 2019 SSW event was discussed in Lim et al. (2021), where they show that the stratospheric polar vortex weakening induced the negative Southern Annular Mode (SAM) phase, which contributed to the Australian drought. Shen et al. (2020) discussed the relations of this event in September 2019 with a blocking situation between 120^0 W and 90^0 W that could increase the amplitude of the planetary waves and contribute to their propagation into the stratosphere. It is known that this propagation has an influence on the stratospheric polar vortex, reducing its intensity at the same time that there is a stratospheric warming (Baldwin et al., 2021). In Fig. 4a (SEP, 2019) the positive geopotential anomaly center over southeastern Pacific Ocean, likely related to a blocking high, is consistent with Shen et al. (2020). In DEC 2019 the SAM negative phase is observed (Fig. 4b), coherent with the results of Rao et al. (2020) who found the impact in the troposphere some months after the SSW occurrence. Fig. 7 shows the vertical structure of temperature and zonal wind anomalies, averaged in longitudes of 120^0 W–360^0 W, from SEP 2019 to MAR 2020. The strong heating in the stratosphere from the pole up to 500 S is observed in SEP 2019, at the same time that there are strong negative zonal wind anomalies, indicating the weakening of the stratospheric polar vortex. In October, November and December 2019 the westerlies weakening extends to the troposphere, resulting in the SAM negative phase in DEC 2019. The anomalous heating displaces from the stratosphere to the troposphere from SEP to DEC and it spreads over SA in the following

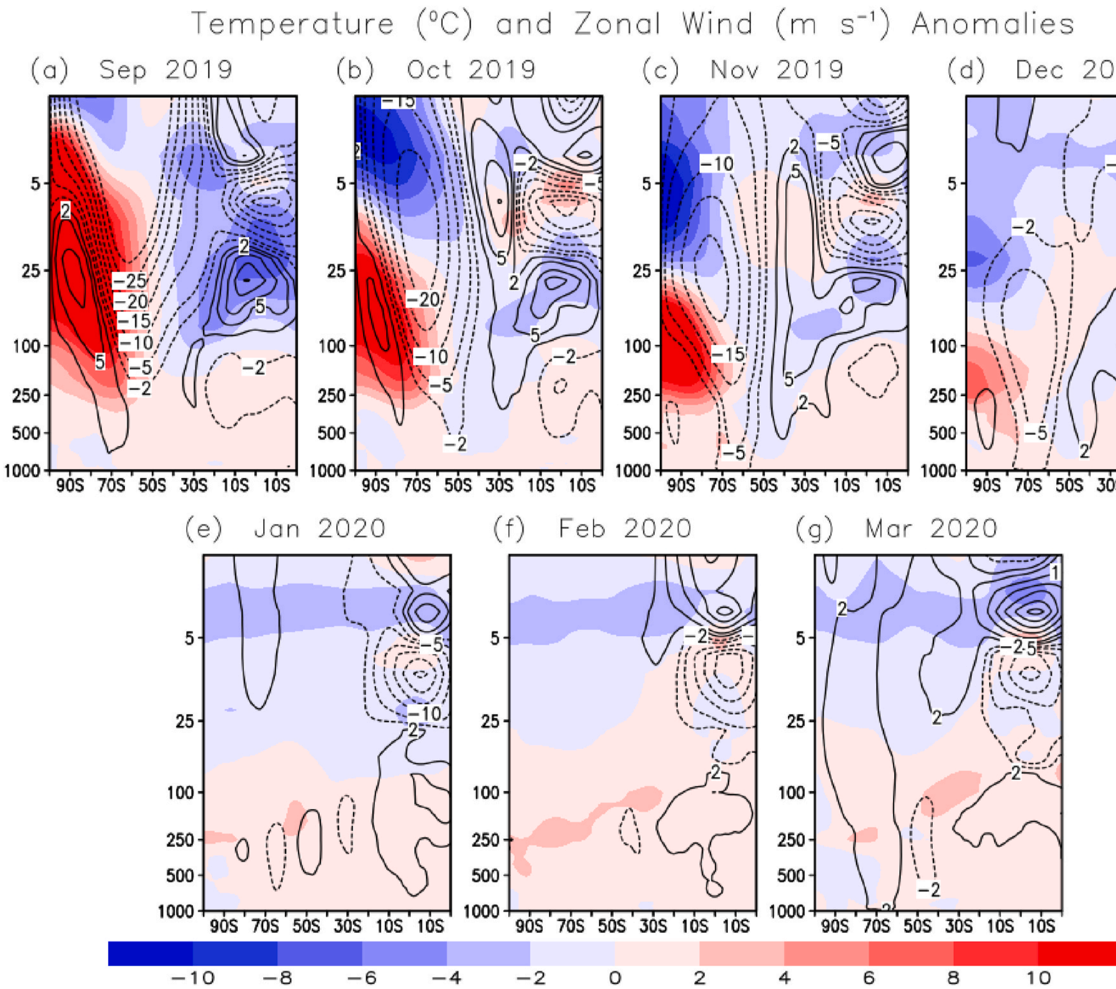

Fig. 7. Vertical structure of temperature anomaly (^{0}C) and zonal wind anomaly (m.s^{-1}) averaged in longitudes of 120^0 W–360^0 W for (a) SEP 2019, (b) OCT, (c) NOV, (d) DEC 2019, (e) JAN 2020, (f) FEB 2020), (g) MAR 2020.

months. The negative SAM phase weakened in JAN and turned positive in MAR. The positive phase indicated by the geopotential average of JAN-FEB-MAR (2020) in Vasconcellos and Souza (2020) was related to the anomalous precipitation in the oceanic SACZ. The SAM influences on SA precipitation have been discussed in Silvestre and Vera (2003), Reboita et al. (2009), Vasconcellos and Cavalcanti (2010), Rosso et al. (2018). These studies show that during summer and positive phase, there is increased precipitation over SE Brazil associated with the SACZ and negative precipitation to the south. During the negative SAM phase there is negative precipitation anomaly in Central-West and Southeast Brazil and positive anomalies to the south. The mechanisms linked to the southern anomalies were related to the northward displacement of the stormtracks and intensification of the subtropical jet or the contribution to intensification of PSA wavetrains. However, during DEC 2019, as other factors were acting, negative precipitation anomalies extended to the south, and the southern sector of Central-West Brazil presented positive anomalies (Fig. 1 b). The positive precipitation anomalies over the ocean suggest that the stormtracks were more active over the Atlantic Ocean. The occurrence of negative SAM, generating subsidence over subtropical areas, was also discussed as a primary driver of extreme dry and hot conditions in Australia during spring 2019 (Lim et al. 2019, 2021). Therefore, the SAM negative phase observed in DEC 2019 could be another contributor for the dry conditions over the observed areas. In MAR 2020 the SAM positive phase was observed (Fig. 4e), which favors dry conditions over SESA.

Other features influenced the drought in SA during the analyzed period. Above normal SSTs were observed in all oceans, mainly in the North Atlantic Ocean, during the whole period of the SA drought. Fig. 8 shows the average of SST anomalies in the longitudes of 70^0 W–35^0 W for each latitude between 18^0 N–34^0 N from January 2019 to September 2020, indicating warmer than normal SST during the drought period. The influence of North Atlantic Ocean SST heating on south of Amazon droughts was discussed in several studies, such as Zeng et al. (2008), Zou et al. (2016), Erfanian et al. (2017). The mechanism is the establishment of a local Hadley cell, with upward motion over the warmer than normal North Atlantic Ocean and subsidence over Amazon. The warmer than normal SST in the North Atlantic has also an influence on the Intertropical Convergence Zone (ITCZ) position, which displaces northwards in this condition (Nobre and Shukla, 1996; Hastenrath, 2006).

Timeseries of precipitation anomalies averaged in Central-West area (65^0 W–50^0 W; 12^0 S–25^0 S) and South area (65^0 W–50^0 W; 25^0 S–35^0 S) are shown in Fig. 9 for SEP and Fig. 10 for MAR. These are months when the 2019/2020 drought spread over the continent (Fig. 1). Figs. 9 and 10 also show the timeseries of DMI, PDO, AMO and El Niño 3.4 indices. Although PDO and AMO have a decadal variability, the indices have also shorter timescale variability.

During the analyzed period, the Atlantic Multidecadal Oscillation (AMO) indicated a positive phase for SEP 2019, SEP 2020 and MAR 2020. It is seen that SEP 2019 and SEP 2020 are years within the five driest years (1988, 2004, 2007, 2019, 2020) in Central-West area and within the four driest years (1987, 2016, 2019, 2020) in South area. MAR 2020 is within the six driest years in Central-West area (1990,

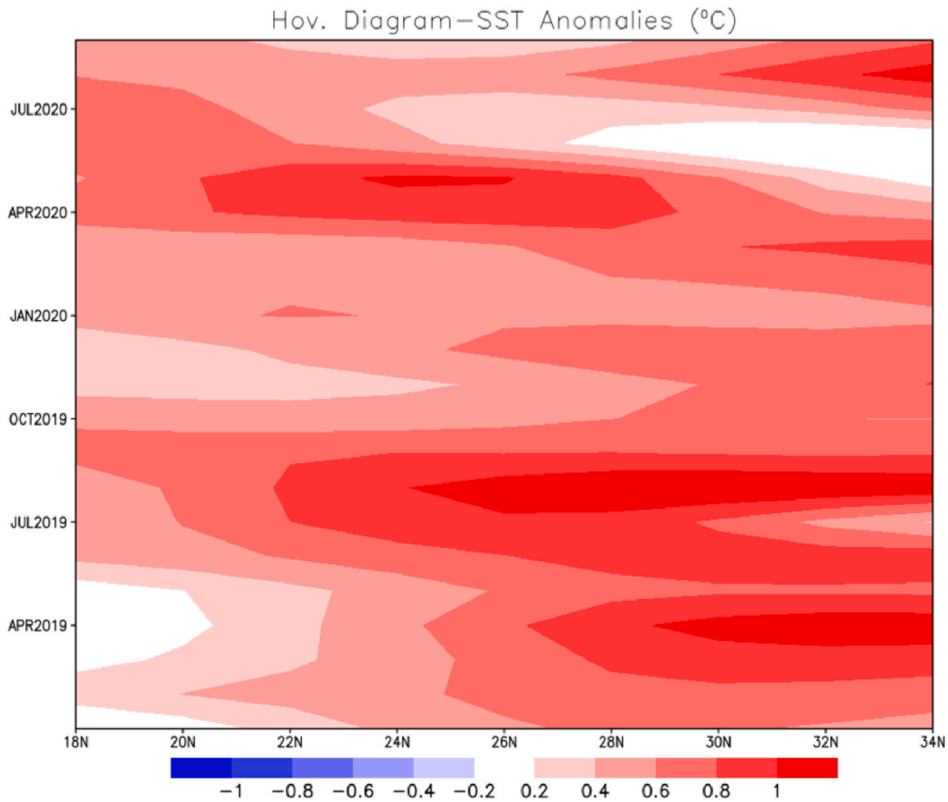

Fig. 8. Hovmöller diagram of SST anomalies (^{0}C) averaged in the longitudes of 70^0 W–35^0 W for each latitude between 18^0 N–34^0 N from January 2019 to September 2020.

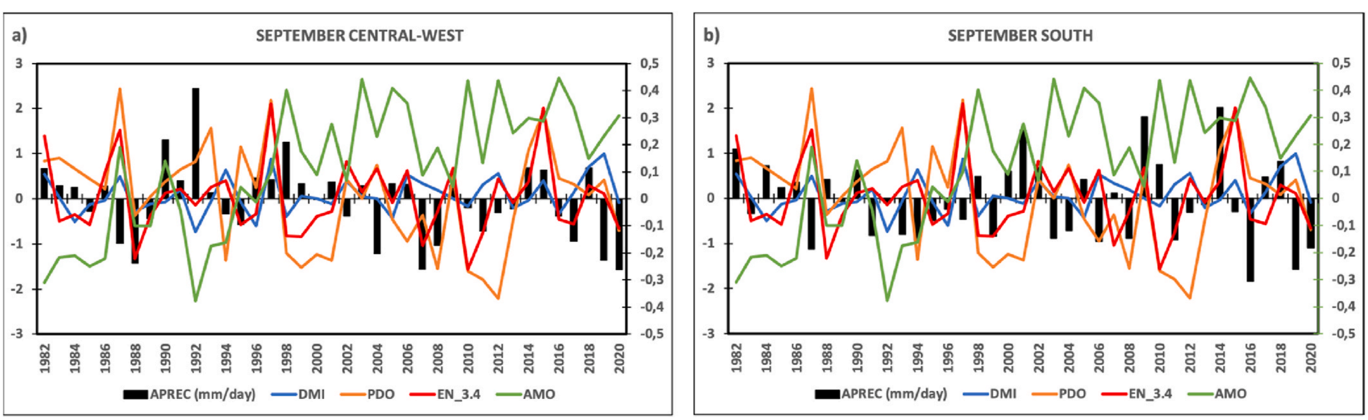

Fig. 9. SEP timeseries of DMI, PDO, EN_3.4, AMO and precipitation anomalies in (a) Central-West area (65^0 W–50^0 W, 12^0 S–25^0 S), (b) South area (65^0 W–50^0 W, 25^0 S–35^0 S).

2002, 2004, 2007, 2012, 2020) and also within the six driest years (1982, 1997, 2004, 2008, 2012, 2020) in the South area. Tables 1–4 show these extreme precipitation years and the sign of the indices. It is seen that unless 1988 and 2016, DMI was positive or neutral when precipitation anomalies were negative in both Central-West and South areas. AMO sign was positive for all years with precipitation anomalies negative in both areas, except 1982, 1988 and 1990. El Niño 3.4 was negative or neutral for the majority of years with negative precipitation anomalies in both areas, except in SEP 2004 and MAR 2020. PDO presented different relations with precipitation anomalies in the two areas. In Central-West the majority of years with negative precipitation anomalies occurred with PDO negative, unless MAR 2004 and SEP 2019. In the South, there were positive or negative PDO in cases of negative precipitation anomalies in SEP and MAR, but in 2020 it was negative in both months.

The Pacific Decadal Oscillation (PDO) index was negative in MAR and SEP 2020 and AMO was positive in MAR 2020, SEP 2019 and SEP 2020. The occurrence of positive AMO phase and negative PDO phase may have intensified the drought over SESA and Central Brazil, as these regions present dry conditions during this combination shown in Kayano

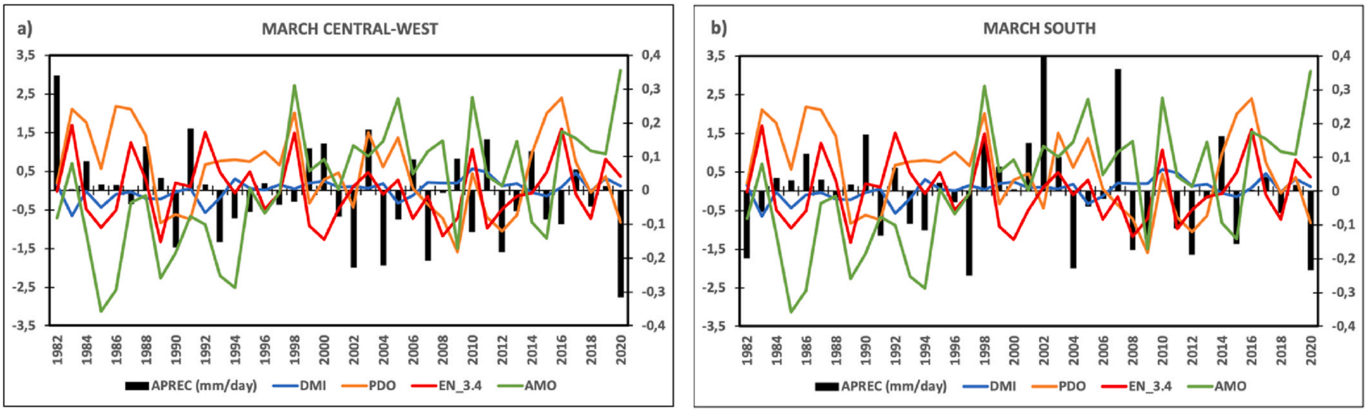

Fig. 10. MAR timeseries of DMI, PDO, EN_3.4, AMO and precipitation anomalies in (a) Central-West area (65⁰ W–50⁰ W, 12⁰ S–25⁰ S), (b) South area (65⁰ W–50⁰ W, 25⁰ S–35⁰ S).

Table 1
Indices in SEP and negative precipitation anomalies in the South (+: positive phase, -: negative phase, n: neutral phase).

	DMI	PDO	EN_3.4	AMO	APREC
1987	+	+	+	+	-
2016	-	+	-	+	-
2019	+	+	n	+	-
2020	n	-	-	+	-

Table 2
Indices in SEP and negative precipitation anomalies in the Central-West (+: positive phase, -: negative phase, n: neutral phase).

	DMI	PDO	EN_3.4	AMO	APREC
1988	-	-	-	-	-
2004	N	n	+	+	-
2007	+	-	-	+	-
2019	+	+	n	+	-
2020	n	-	-	+	-

Table 3
Indices in MAR and negative precipitation anomalies in the Central-West (+: positive phase, -: negative phase, n: neutral phase).

	DMI	PDO	EN_3.4	AMO	APREC
1990	n	-	n	-	-
2002	n	-	n	+	-
2004	n	+	n	+	-
2007	+	-	-	+	-
2012	+	-	-	+	-
2020	+	-	+	+	-

Table 4
Indices in MAR and negative precipitation anomalies in the SOUTH (+: positive phase, -: negative phase, n: neutral phase).

	DMI	PDO	EN_3.4	AMO	APREC
1982	n	n	n	-	-
1997	+	+	n	+	-
2004	+	+	n	+	-
2008	+	-	-	+	-
2012	+	-	-	+	-
2020	+	-	+	+	-

et al. (2019). The Dipole Mode Index (DMI), which represents the Indian Ocean Dipole (IOD), was positive and high in SEP 2019 and MAR 2020 and could have contributed to the establishment of a wavetrain over Indian and Pacific Oceans that reached South America. The influence of the IOD on South American climate was discussed by Saji et al. (2005), who showed positive correlations between IOD and land surface temperature over subtropical SA, and by Chan et al. (2008), who found reduced precipitation over central Brazil associated with positive IOD.

Correlations of these indices with precipitation anomalies are shown in Fig. 11 (SEP) and Fig. 12 (MAR). The negative correlations between the AMO index and precipitation anomalies over Amazon, Central-West and Southeast Brazil (Fig. 11 a) illustrate the relation between North Atlantic positive SST anomalies and dry conditions over SA in SEP. Positive correlations of EN_3.4 index or PDO with precipitation anomalies in Central-West area (Central and Southeast) in SEP indicate dry conditions in these areas in La Niña events and negative PDO (Fig. 11 b, d). Negative correlations in areas of SA between DMI and precipitation anomalies are consistent with dry conditions in the positive phase (Fig. 11 c). In MAR, there are negative correlations in some areas with DMI and AMO, and positive with EN 3.4 and PDO in the south, but only small areas with significant correlations (Fig. 12).

The occurrence of a canonical La Nina event in the second half of 2020 (negative EN_3.4 in SEP, 2020), which persisted up to the beginning of 2021 contributed to the continuity of the SA drought, mainly in southern Brazil, illustrated by the precipitation anomalies in SEP 2020 (Fig. 1f). The influence of ENSO events on southern Brazil was discussed by Grimm et al. (2000), and several studies showed the relation between canonical La Niña occurrence and negative precipitation anomalies over Southern Brazil (Tedeschi et al., 2013). The typical cyclonic circulation anomaly at high levels over east Tropical Pacific Ocean during La Niña events is seen in Fig. 4f. This anomaly induces the wavetrain towards south of SA, which then turns northwards, establishing an anticyclonic circulation and positive geopotential anomalies over the regions where there are negative precipitation anomalies (Figs. 4f and 1f).

5. Conclusion

The paper describes the impacts of the 2019/2020 drought on agriculture, water resources and fires in Brazil, Argentina, Paraguay and Uruguay and discusses the atmospheric and oceanic features that contributed to the extended dry period in these regions. The drought reduced the crops, reduced the river levels, affecting the fluvial transportation, and reduced the hydropower generation. The high temperatures and the reduction of humidity in some months also had a negative impact, causing extensive and intense fires in many regions of SA.

The analyses showed that there were several processes that contributed to the drought, different from other dry years in SA, for example, 2014 and 2015 (Coelho et al., 2016; Cavalcanti et al., 2017). In those cases, there were influences of wavetrains triggered by convection in the western tropical Pacific Ocean on the establishment of a high pressure center anomaly over southeastern SA, responsible for the dry

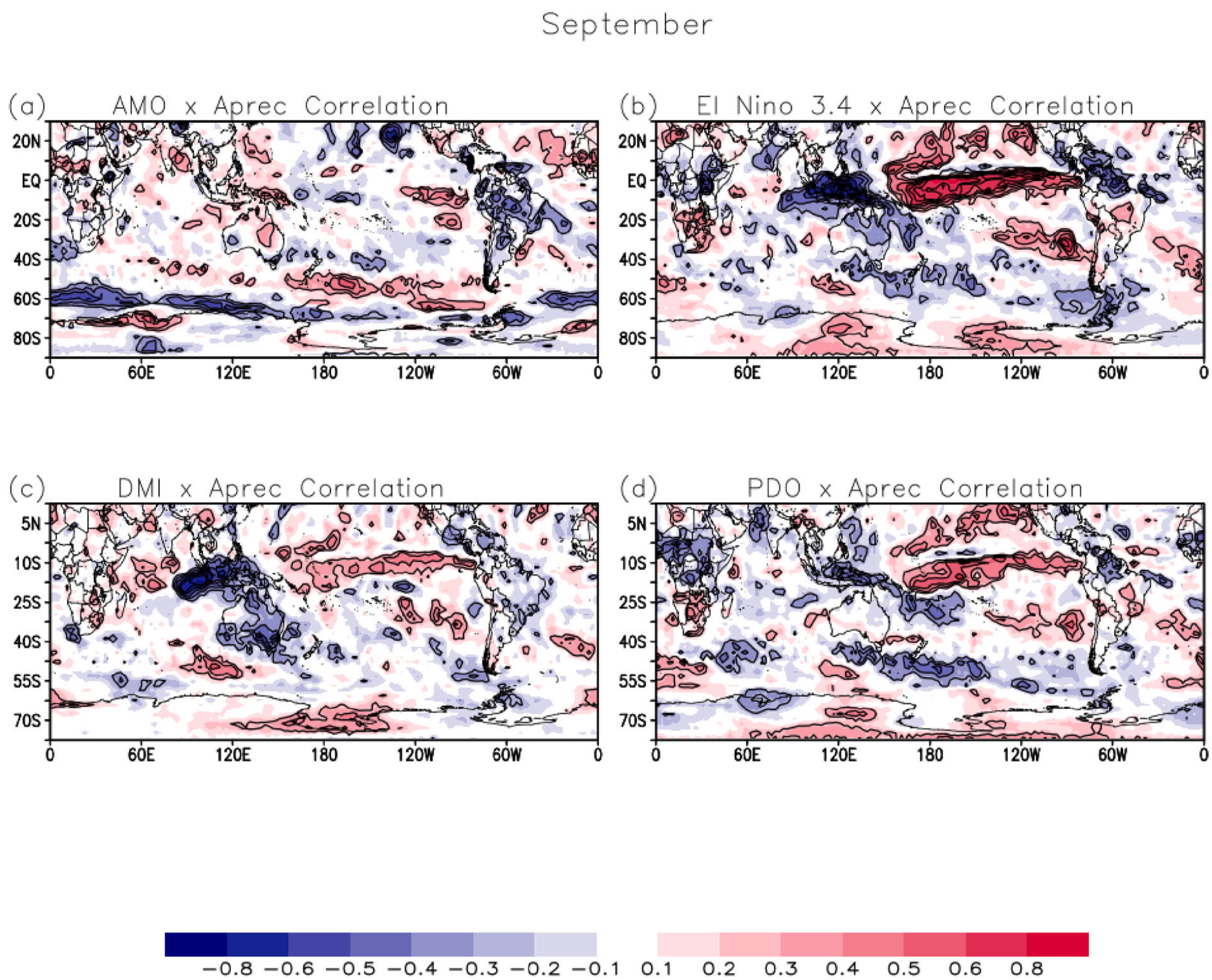

Fig. 11. Correlations between indices and precipitation anomalies in SEP (a) AMO, (b) El Niño 3.4, (c) DMI, (d) PDO. Contours indicate the areas with significance level less than 0.1.

conditions. Another extreme drought over the SA monsoon region in 2001 was related to a large number of cyclonic vortices at high levels, which displaced from the tropical Atlantic Ocean to the region, and to wavetrains over the Pacific Ocean linked to tropical convection anomalies (Cavalcanti and Kousky, 2001).

In the present case, many features were observed during the period, summarized as follows. There were steady conditions of convection anomalies in the Tropical Western Pacific Ocean, which contributed to the steady conditions over SA and over the Atlantic Ocean. There was occurrence of the SSW, which resulted in the negative phase of SAM and also the heating propagation to the troposphere. The warm North Atlantic Ocean SSTs in 2019/2020 contributed to the dry conditions over Amazon and central SA, consistent also with Marengo et al. (2021) who associated the anomalous North Atlantic Ocean warming with the 2010 and 2019 droughts. The North Atlantic positive anomalies could be associated with the Atlantic Multidecadal Oscillation (AMO) positive phase. AMO influence on the 2020 drought in southern Brazil was also indicated by Grimm et al. (2020) as a contributor to the extreme observed dry conditions. Chen et al. (2011) related fires in southern Amazon to the AMO positive phase, associating this phase with dry conditions. Another driver of the observed drought in SA could be the occurrence of an extreme Indian Ocean Dipole (IOD) in the positive phase during SON 2019, also discussed by Du et al. (2020). These influences occur through a wavetrain from the Indian Ocean to SA. Therefore, this event could have contributed to the dry conditions over SA in 2019 spring. During the months of JAN, FEB and MAR, while there were dry conditions in Central-West and South areas, there was excessive precipitation over parts of Southeast, associated with an oceanic SACZ, that was intensified by the stationary trough over southwest South Atlantic and by the South Atlantic SST gradient between tropical-subtropical regions.

All these large scale aspects, along with the PDO negative phase and occurrence of a canonical La Niña event in the second semester of 2020, contributed to the development and extended period of dry conditions over SA during the analyzed period causing what is to date, the most widespread drought in time and space that has affected large regions of the continent.

Declaration of competing interest

The authors declare that they have no known competing financial interests or personal relationships that could have appeared to influence the work reported in this paper.

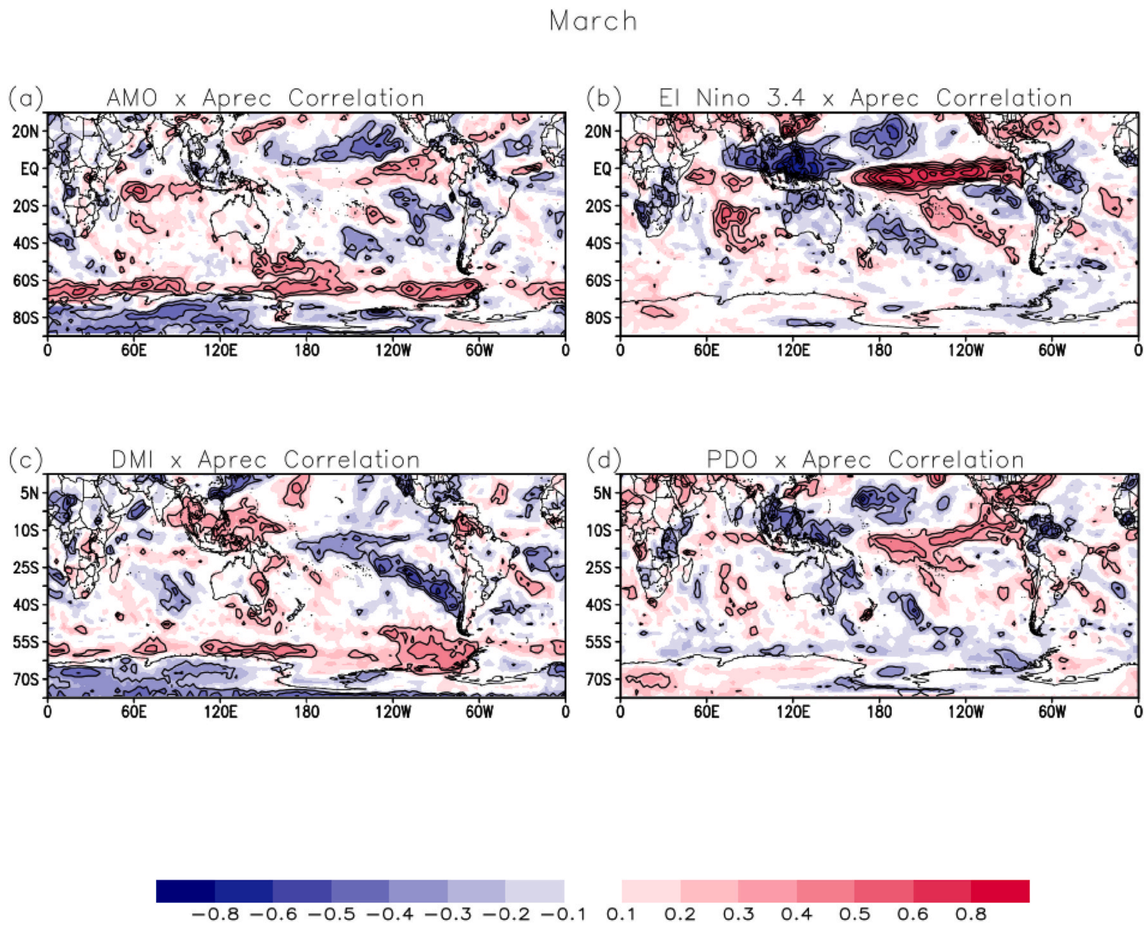

Fig. 12. Correlations between indices and precipitation anomalies in MAR (a) AMO, (b) El Niño 3.4, (c) DMI, (d) PDO. Contours indicate the areas with significance level less than 0.1.

Acknowledgements

To Fundação de Amparo à Pesquisa do Estado de São Paulo (FAPESP)-Belmont Forum -CLIMAX-2015/50687-8 and Coordenação de Aperfeiçoamento de Pessoal de Nível Superior (CAPES)- 88887.469114/2019-00). IFAC thanks Conselho Nacional de Desenvolvimento Científico e Tecnológico (CNPq) project 306393/2018-2, CASC thanks CNPq, project 305206/2019-2 and DCS was supported by CAPES project 88887.469114/2019-00.

References

Adler, R.F., Sapiano, M.R.P., Huffman, G.J., Wang, J.-J., Gu, G., Bolvin, D., Chiu, L., Schneider, U., Becker, A., Nelkin, E., Xie, P., Ferraro, R., Shin, D.-B., 2018. The Global Precipitation Climatology Project (GPCP) monthly analysis (new version 2.3) and a review of 2017 global precipitation. Atmosphere 9 (4), 138. https://doi.org/10.3390/atmos9040138.

AP News, 2020. Available at: https://apnews.com/article/droughts-caribbean-brazil-paraguay-latin-america-f7538b9e0d499a4d27961a2fae3f18ce.

Aragão, Luiz E., Silva Junior, O.C., Celso, H.L., Anderson, Liana O., 2020. Brazil's challenge to restrain deforestation and fires in the Amazon during COVID-19 pandemic in 2020. Environmental, social implications and their governance. São José dos Campos 34. https://doi.org/10.13140/RG.2.2.17256.49921. SEI/INPE: 01340.004481/2020-96/5543324.

Arraut, J.M., Nobre, C., Barbosa, H.M.J., Obregon, G., Marengo, J.A., 2012. Aerial rivers and lakes: looking at large-scale moisture transport and its relation to Amazonia and to subtropical rainfall in South America. J. Clim. 25, 543–556. https://doi.org/10.1175/2011JCLI4189.1, 2012.

Baldwin, M.P., Ayarzaguena, B., Birner, T., Butchart, N., Butler, A.H., Charlton-Perez, A. J., Domeisen, D.I.V., Garfinkel, C.I., Garny, H., Gerber, E.P., Hegglin, M.I., Langematz, U., Pedatella, N.M., 2021. Sudden stratospheric warmings. Rev. Geophys. 59, e2020RG000708 https://doi.org/10.1029/2020RG000708.

Barreto, N.J.C., Cavalcanti, I.F.A., Mesquita, M.d.S., Pedra, G.U., 2019. Multivariate intraseasonal rainfall index applied to South America. Meteorol. Appl. 26, 521–527. https://doi.org/10.1002/met.1780.

BCBA, 2020. Bolsa de Cereales de Buenos Aires. In: Informe de cierre de campaña. Departamento de estimaciones agrícolas, Instituto de Estudios Económicos, Buenos Aires Argentina. Available at : http://bibliotecadigital.bolsadecereales.com.ar/greenstone/collect/pubper/index/assoc/HASH16e9/63d59d17.dir/CC2020.,%20jun.pdf.

BCR, 2020. Bolsa de Comercio de Rosario (in Spanish). In: Río Paraná: la bajante más severa en los últimos 50 años representa un costo de US$ 244 millones para el complejo agroexportador. Available at: https://bcr.com.ar/es/sobre-bcr/medios/noticias/rio-parana-la-bajante-mas-severa-en-los-ultimos-50-anos-representa-un.

Carvalho, L.M.V., Jones, C., Liebmann, B., 2004. The South Atlantic convergence zone: persistence, intensity, form, extreme precipitation, and relationships with intraseasonal to interannual activity and extreme rainfall. J. Clim. 17, 88–108.

Carvalho, L.M.V., Silva, A.E., Jones, C., Liebmann, B., Dias, P.L.S., Rocha, H.R., 2011. Moisture transport and intraseasonal variability in the South America monsoon system. Clim. Dynam. 36, 1865–1880. https://doi.org/10.1007/s00382-0100806-2.

Carvalho, L.M.V., Cavalcanti, I.F.A., 2016. The South American Monsoon System (SAMS). In: de Carvalho, L., Jones, C. (Eds.), The Monsoons and Climate Change. Springer Climate. https://doi.org/10.1007/978-3-319-21650-8_6.

Cavalcanti, I.F.A., Kousky, V.E., 2001. Drought in Brazil during summer and fall 2001 and associated atmospheric circulation features. Revista Climanálise 2, 1–10. Available at: http://urlib.net/cptec.inpe.br/walmeida/2004/12.07.14.17.

Cavalcanti, I.F.A., Marengo, J.A., Alves, L.M., Costa, D.F., 2017. On the opposite relation between extreme precipitation over west Amazon and southeastern Brazil: observations and model simulations. Int. J. Climatol. 37, 3606–3618. https://doi.org/10.1002/joc.4942.

Chan, S.C., Behera, S.K., Yamagata, T., 2008. Indian Ocean Dipole influence on south American rainfall. Geophys. Res. Lett. 35, L14S12. https://doi.org/10.1029/2008GL034204.

Chen, Y., Randerson, J.T., Morton, D.C., DeFries, R.S., Collatz, J., Kasibhatla, P.S., Giglio, L., Jin, Y., Marlier, M.E., 2011. Forecasting fire season severity in South America using sea surface temperature anomalies. Science 334 (6057), 787–791. https://doi.org/10.1126/science.1209472.

CEMADEN - Centro Nacional de Monitoramento e Alertas de Desastres Naturais. Boletim Monitoramento de secas e impactos no Brasil Abril, 2020. Ano 03. Número 18. Ministério da Ciência, Tecnologia e Inovações. Brasil.

Clarín, 2020. Extraño fenómeno. Por la invasión de algas verdes en el Río de la Plata, casi la mitad de los platenses está sin agua potable. Available at: https://www.clarin.com/ciudades/invasion-algas-verdes-rio-plata-mitad-platenses-agua-potable_0_WyDrGUmhl.html.

Coelho, C.A.S., de Oliveira, C.P., Ambrizzi, T., Reboita, M.S., Carpenedo, C.B., Campos, L.P.S., Tomaziello, A.C.N., Pampuch, L.A., Custódio, M.S., Dutra, L.M.M., da Rocha, R.P., Rehbein, A., 2016. The 2014 southeast Brazil austral summer drought: regional scale mechanisms and teleconnections. Clim. Dynam. 46, 3737–3752. https://doi.org/10.1007/s00382-015-2800-1.

Cunningham, C.A.C., Cavalcanti, I.F.A., 2006. Intraseasonal modes of variability affecting the south atlantic convergence zone. *Int. J. Climatol.*: A Journal of the Royal Meteorological Society 26, 1165–1180. https://doi.org/10.1002/joc.1309.

DERAL – Departamento de Economia Rural, 2020. Boletim Informativo – Estiagem Histórica no Paraná – Maio de. Available at. https://www.agricultura.pr.gov.br/sites/default/arquivos_restritos/files/documento/2020-05/estiagem_18_maio_2020.pdf.

DMH - Dirección de Meteorología e Hidrología de Paraguay. Informe hidrometeorológico conjunto del río Paraguay. Date: 01-06-2020.

Du, Y., Zhang, Y., Zhang, L.-Y., Tozuka, T., Ng, B., Cai, W., 2020. Thermocline warming induced extreme Indian Ocean dipole in 2019. Geophys. Res. Lett. 47, e2020GL090079 https://doi.org/10.1029/2020GL090079.

EPAGRI – CEPA, 2020. Available at. https://cepa.epagri.sc.gov.br/.

Erfanian, A., Wang, G., Fomenko, L., 2017. Unprecedented drought over tropical South America in 2016: significantly under-predicted by tropical SST. Sci. Rep. 7, 5811. https://doi.org/10.1038/s41598-017-05373-2.

Grimm, A.M., Barros, V.R., Doyle, M.R., 2000. Climate variability in southern south America associated with El Niño and La Niña events. J. Clim. 13, 35–58. https://doi.org/10.1175/1520-0442(2000)013<0035:CVISSA>CO2.

Grimm, A.M., Zilli, M.T., 2009. Interannual variability and seasonal evolution of summer monsoon rainfall in South America. J. Clim. 22, 2257–2275. https://doi.org/10.1175/2008JCLI2345.1.

Grimm, A.M., Almeida, A.S., Beneti, C.A.A., Leite, E.A., 2020. The combined effect of climate oscillations in producing extremes: the 2020 drought in southern Brazil. Brazilian Journal of Water Resources 25, e48. https://doi.org/10.1590/2318-0331.252020200116.

Hastenrath, S., 2006. Circulation and teleconnection mechanisms of Northeast Brazil droughts. Prog. Oceanogr. 70, 407–415. https://doi.org/10.1016/j.pocean.2005.07.004.

Hersbach, H., Bell, B., Berrisford, P., Hirahara, S., Horányi, A., Muñoz-Sabater, J., Nicolas, J., Peubey, C., Radu, R., Schepers, D., Simmons, A., Soci, C., Abdalla, S., Abellan, X., Balsamo, G., Bechtold, P., Biavati, G., Bidlot, J., Bonavita, M., De Chiara, G., Dahlgren, P., Dee, D., Diamantakis, M., Dragani, R., Flemming, J., Forbes, R., Fuentes, M., Geer, A., Haimberger, L., Healy, S., Hogan, R.J., Hólm, E., Janisková, M., Keeley, S., Laloyaux, P., Lopez, P., Lupu, C., Radnoti, G., de Rosnay, P., Rozum, I., Vamborg, F., Villaume, S., Thépaut, J.-N., 2020. The ERA5 global reanalysis. Q. J. R. Meteorol. Soc. 146, 1999–2049. https://doi.org/10.1002/qj.3803.

Huang, B., Thorne, P.W., Banzon, V.F., Boyer, T., Chepurin, G., Lawrimore, J.H., Menne, M.J., Smith, T.M., Vose, R.S., Zhang, H.-M., 2017. Extended reconstructed sea surface temperature, version 5 (ERSSTv5): upgrades, validations, and intercomparisons. J. Clim. 30, 8179–8205. https://doi.org/10.1175/JCLI-D-16-0836.1.

INA, 2020. Instituto Nacional del Agua (in Spanish). In: Alerta Hidrológico Cuenca del Plata: Informes MENSUALES Emitidos. Available at: https://www.ina.gov.ar/alerta/index.php?seccion=2&year=2020.

INPE, Instituto Nacional de Pesquisas Espaciais, 2020. Monitoramento dos Focos Ativos por Países. Instituto Nacional de Investigaciones Espaciales. Available at: http://queimadas.dgi.inpe.br/queimadas/portal-static/estatisticas_paises/.

Kayano, M.T., Andreoli, R.V., Souza, R.A.F.D., 2019. El Niño–southern oscillation related teleconnections over South America under distinct Atlantic multidecadal oscillation and Pacific Interdecadal oscillation backgrounds: La Niña. Int. J. Climatol. 39, 1359–1372. https://doi.org/10.1002/joc.5886.

La Nación, 2020. Dragado no está teniendo la eficiencia necesaria y suma pérdidas a las importaciones. Available at: https://www.lanacion.com.py/negocios/2020/10/14/dragado-no-esta-teniendo-la-eficiencia-necesaria-y-suma-perdidas-a-las-importaciones/.

Lee, H.-T., NOAA CDR Program, 2018. NOAA Climate Data Record (CDR) of Monthly Outgoing Longwave Radiation (OLR), Version 2.7. NOAA National Centers for Environmental Information. https://doi.org/10.7289/V5.

Lim, E.-P., Hendon, H.H., Boschat, G., Hudson, D., Thompson, D.W.J., Dowdy, A.J., Arblaster, J.M., 2019. Australian hot and dry extremes induced by weakenings of the stratospheric polar vortex. Nat. Geosci. 12, 896–901. https://doi.org/10.1038/s41561-019-0456-x.

Lim, E.-P., Hendon, H.H., Butler, A.H., Thompson, D.W.J., Lawrence, Z., Scaife, A.A., Shepherd, T.G., Polichtchouk, I., Nakamura, H., Kobayashi, C., Comer, R., Coy, L., Dowdy, A., Garreaud, R.D., Newman, P.A., Wang, G., 2021. The 2019 Southern Hemisphere stratospheric polar vortex weakening and its impacts. Bull. Am. Meteorol. Soc. 1–50. https://doi.org/10.1175/BAMS-D-20-0112.1.

Madden, R.A., Julian, P.R., 1972. Description of global-scale circulation cells in the tropics with a 40–50 day period. J. Atmos. Sci. 29, 1109–1123. https://doi.org/10.1175/1520-0469(1972)029<1109:DOGSCC>2.0.CO;2.

MAGyP, 2020. Informe de Sequía. Septiembre 2020 (Fecha de elaboración 29/09/2020). Ministerio de Agricultura, Ganadería y Pesca. Available at: https://www.magyp.gob.ar/sitio/areas/d_eda/sequia/_archivos//000000_Informes/200900_2020_09_SEQUIA.pdf.

Marengo, J.A., Soares, W.R., Saulo, C., Nicoloni, M., 2004. Climatology of the low-level jet east of the Andes as derived from the NCEP–NCAR reanalyses: characteristics and temporal variability. J. Clim. 17, 2261–2280. https://doi.org/10.1175/1520-0442(2004)017<2261:COTIJE>2.0.CO;2.

Marengo, J.A., Liebmann, B., Grimm, A.M., Misra, V., 2012. Recent developments on the South American monsoon system. Int. J. Climatol. 32, 1–21. https://doi.org/10.1002/joc.2254.

Marengo, J.A., Cunha, A.P., Cuartas, L.A., Leal, K.R.D., Broedel, E., Seluchi, M.E., Michelin, C.M., Baião, C.F.P., Ângulo, E.C., Almeida, E.K., Kazmierczac, M.L., Mateus, N.A.P., Silva, R.C., Bender, F., 2021. Extreme drought in the Brazilian pantanal in 2019–2020: characterization, causes, and impacts. Frontiers in Water 3, 639204. https://doi.org/10.3389/frwa.2021.639204.

Martinez, J.A., Dominguez, F., 2014. Sources of atmospheric moisture for the La Plata river basin. J. Clim. 27, 6737–6753. https://doi.org/10.1175/JCLI-D-14-00022.1.

Mo, K.C., Paegle, J.N., 2001. The Pacific-South American modes and their downstream effects. Int. J. Climatol. 21, 1211–1229. https://doi.org/10.1002/joc.685.

NASA, 2020a. NASA Earth Observatory. In: Severe Drought in South America. Available at: https://earthobservatory.nasa.gov/images/147480/severe-drought-in-southamerica.

NASA, 2020b. NASA Earth Observatory. In: Fires Char the Pantanal. Available at: https://earthobservatory.nasa.gov/images/147269/fires-char-the-pantanal.

Nobre, P., Shukla, J., 1996. Variations of sea surface temperature, wind stress, and rainfall over the tropical atlantic and south America. J. Clim. 9, 2464–2479.

OPYPA, 2020. Análisis Sectorial Y Cadenas Productivas. https://descargas.mgap.gub.uy/OPYPA/Anuarios/anuario2020/anuario2020.pdf.

Rao, J., Garfinkel, C.I., White, I.P., Schuartz, 2020. The southern hemisphere minor sudden stratospheric warming in september 2019 and its predictions in S2S models. J. Geophys. Res.: Atmosphere 125, 1–19. https://doi.org/10.1029/2020JD032723.

Reboita, M.S., Ambrizzi, T., Rocha, R.P., 2009. Relationship between the southern annular mode and southern hemisphere atmospheric systems. Revista Brasileira de Meteorologia. São Paulo 24, 48–55. https://doi.org/10.1590/S0102-77862009000100005.

Rosa, E.B., Pezzi, L.P., Quadro, M.F.L., Brunsell, N., 2020. Automated detection algorithm for SACZ, oceanic SACZ, and their climatological features. Frontiers in Environmental Science 8, 18. https://doi.org/10.3389/fenvs.2020.0001.

Rosso, F.V., Boiaski, N.T., Ferraz, S.E.T., Robles, T.C., 2018. Influence of the antarctic oscillation on the south atlantic convergence zone. Atmosphere 9 (11), 431. https://doi.org/10.3390/atmos9110431.

Saji, N.H., Ambrizzi, T., Ferraz, S.E.T., 2005. Indian Ocean Dipole mode events and austral surface air temperature anomalies. Dynam. Atmos. Oceans 39, 87–101. https://doi.org/10.1016/j.dynatmoce.2004.10.015. ISSN0377-0265.

Schubert, S.D., Suarez, M.J., Pegion, P.J., Koster, R.D., Bacmeister, J., 2004. Causes of long-term drought in the US great plains. J. Clim. 17, 485–503. https://doi.org/10.1175/1520-0442(2004)017%3c0485:COLDIT%3e2.0.CO;2.

Shen, X., Wang, L., Osprey, S., 2020. Tropospheric forcing of the 2019 Antarctic sudden stratospheric warming. Geophys. Res. Lett. 47, e2020GL089343 https://doi.org/10.1029/2020GL089343.

Silvestre, G.E., Vera, C.S.(, 2003. Antarctic Oscillation signal on precipitation anomalies over southeastern South America. Geophys. Res. Lett. 30, 2115–2118. https://doi.org/10.1029/2003GL018277.

SMN - Servicio Meteorológico Nacional, 2021. Reporte - Estado del clima en Argentina 2020. Argentina. SMN y Ministerio de Defensa de Argentina.

SNMF- Servicio Nacional de Manejo del Fuego, 2020. Available at: https://www.argentina.gob.ar/ambiente/manejo-del-fuego.

Tedeschi, R.G., Cavalcanti, I.F.A., Grimm, A.M., 2013. Influences of two types of ENSO on South American precipitation. Int. J. Climatol. 33, 1382–1400. https://doi.org/10.1002/joc.3519.

Telam, 2020. Las aguas del Río de la Plata presentan una tonalidad verdosa por la presencia de cianobacterias. Available at: https://www.telam.com.ar/notas/202011/534827-aguas-verdes-rio–de–la-plata.html.

Vasconcellos, F.C., Cavalcanti, I.F.A., 2010. Extreme precipitation over Southeastern Brazil in the austral summer and relations with the Southern Hemisphere annular mode. Atmos. Sci. Lett. 11, 21–26. https://doi.org/10.1002/asl.247.

Vasconcellos, F.C., Souza, J.N., 2020. The anomalous wet 2020 southeast Brazil austral summer: characterization and possible mechanisms. Atmósfera. https://doi.org/10.20937/ATM.52919.

Wilhite, D., Glantz, M., 1985. Understanding the drought phenomenon: the role of definitions. Water Int. 10, 111–120. https://doi.org/10.1080/02508068508686328.

Wilhite, D.A., 2012. Series preface — drought and water crises. Drought Mitigation Center Faculty Publications 108. http://digitalcommons.unl.edu/droughtfacpub/108.

Zeng, N., Yoon, J.-H., Marengo, J.A., Subramaniam, A., Nobre, C.A., Mariotti, A., Neelin, J.D., 2008. Causes and impacts of the 2005 Amazon drought. Environ. Res. Lett. 3, 014002 https://doi.org/10.1088/1748-9326/3/1/014002.

Zou, Y., Macau, E.E.N., Sampaio, G., Ramos, A.M.T., Kurths, J., 2016. Do the recent severe droughts in the Amazonia have the same period of length? Clim. Dynam. 46, 3279–3285. https://doi.org/10.1007/s00382-015-2768-x.